Friction https://mc03.manuscriptcentral.com/friction
https://doi.org/10.26599/FRICT.2026.9441214

Research Article

Study on the effect of diketone lubricant on the tribological properties of angular contact ball bearing with skidding behavior

Shaonan Du[1], Chenhui Zhang[2*], Zhi Luo[3]

[1] *School of Energy Power and Mechanical Engineering, North China Electric Power University, Beijing 102206, China*

[2] *State Key Laboratory of Tribology in Advanced Equipment, Tsinghua University, Beijing 100084, China*

[3] *Beijing National Laboratory of Molecular Sciences, CAS Key Laboratory of Engineering Plastics, Institute of Chemistry, Chinese Academy of Sciences, Beijing 100190, China*

* Corresponding author: Chenhui Zhang, E-mail: chzhang@tsinghua.edu.cn.

Received: July 21, 2025; Revised: November 2, 2025; Accepted: January 5, 2026

Abstract: Skidding in angular contact ball bearings can significantly increase friction, wear and temperature, affecting bearing performance and service life. Despite its important impact, few studies have systematically investigated lubrication behavior under skidding conditions, where conventional lubricants often fail to provide stable low-friction operation. To address this issue, this study first calculated the critical skidding parameters of angular contact ball bearings using a quasi-static model. Then, experimental parameters of bearings with skidding and non-skidding were selected to study their tribological behaviors under lubrication with three different lubricants (base oil, commercial lubricant, and diketone lubricant). The study found that when the bearing had skidding behavior, the lowest friction coefficient and temperature rise (0.0008, 2.8℃) can be achieved only under lubrication with PAO=14(20%) (diketone lubricant). In addition, the bearings lubricated with diketone show excellent anti-wear performance and extremely short running-in period. The mechanism of the excellent tribological performance of diketone-based lubricants came from the synergistic effect of diketone molecular adsorption layer and chelation, which can reduce friction and temperature rise. These findings highlight the potential of diketone lubricants to improve bearing performance and durability under extreme operating conditions.

Keywords: Angular contact ball bearing; Tribological properties; Superlubricity; Diketone; Skidding behavior

1 Introduction

Rolling bearings are indispensable key components in mechanical equipment. Angular contact ball bearings are widely used in aerospace, CNC machine tools, precision instruments and automotive industries due to their unique axial and radial load-bearing capacity and high rotation accuracy. These bearings are typically oil-lubricated to ensure effective heat dissipation and precise lubrication at high speeds [1]. The lubrication state and performance directly influence friction and wear reduction, transmission efficiency, and the prevention of surface fatigue caused by lubricant film rupture. In the actual operation, local skidding often arises from relative speed difference between the balls and the raceways, especially under light loads and high-speed conditions [2, 3]. For example, wind turbine gearbox bearing, high-speed motors, precision machine tool bearings, etc. all have serious skidding problems [4-6]. Skidding increases local contact stress, disrupts the lubricant film, and leads to surface adhesive wear, fatigue pitting, and material spalling [7]. In addition, the ball may produce instantaneous high temperature during the skidding process, which accelerates the oxidation of the lubricant and aggravates the lubrication failure [8].

Extensive research has been conducted on the skidding phenomenon in angular contact ball bearings through theoretical analysis, numerical simulation, and experimental investigation. In the aspect of theoretical research, the mathematical model of skidding mechanism was established, and the influence of sliding friction, lubrication state and load distribution on skidding was discussed [9, 10]. Finite element simulations under various operating conditions have revealed that axial load and lubricant viscosity significantly influence the skidding rate [11, 12]. In the aspect of experimental research, the researchers used high-speed bearing test bench, high-speed camera technology and surface topography analysis methods to study the skidding phenomenon under different working conditions [13-15]. For example, Fang et al. [16] established a model to estimate heat generation due to skidding and validated its impact on outer ring temperature rise (TMR) under varying preload and speed using a bearing test rig. Gao et al. [17] developed a high-precision, self-powered triboelectric bearing skidding sensor (HP-TEBSS) capable of real-time skidding detection, and demonstrated that skidding severity increases with speed under light loads. In addition, studies had found that under high-speed rotation conditions, high-performance synthetic lubricants containing additives can significantly reduce the friction, wear and TMR of bearings under high skidding levels compared to traditional mineral oils [18, 19]. These findings underscored the critical influence of lubricant properties on the tribological behavior of angular contact ball bearings and highlighted the potential of advanced lubricants to mitigate skidding-related damage.

Since the superlubricity was proposed in the last century, it has achieved remarkable research results after nearly 40 years of development [20-23]. In particular, the research on oil-based superlubricity in the past 10 years has provided a new solution to the friction and wear problems that have been plaguing the field of mechanical engineering [24]. Traditional mineral lubricants or fully synthetic lubricants have high viscosity or long molecular chains, resulting in high viscous friction of lubricants [25]. Therefore, it was difficult to achieve oil-based superlubricity on the metal friction pairs even under full-film lubrication [26]. In order to reduce the viscous resistance of the lubricant, researchers had found that diketone lubricants with liquid crystal-like structure can not only formed ordered molecular layers under shear induction, making the molecular contact between friction surfaces more regular and smooth [27], but also formed a stable molecular adsorption film by chemical reaction with metal friction pairs [28], so as to achieve the purpose of isolating direct contact between friction pairs. The above research results show that the diketone lubricant can make the metal friction pair exhibit macroscopic superlubricity (sliding friction coefficient < 0.01), but it brought high wear (contact pressure less than 50 MPa). To clarify the role of chelates in achieving superlubricity, our research group conducted preliminary research on the synergistic lubrication of diketones and chelates. We determined that chelate formation was the primary driver of superlubricity and wear reduction, further refining the superlubricity mechanism of diketones [29]. Subsequently, we conducted tribological studies on lubricants formulated with diketones and base oils, determining the optimal blend ratio of diketones, chelates, and PAOs. This mixed lubricant further increased the contact pressure (increased by 222%, up to 161 MPa) of friction pairs achieving superlubricity and shortened the running-in time (decreased by 53.3%) [30]. These results highlighted the importance of minimizing metal loss on contact surfaces and enhancing oil film load-bearing capacity in achieving stable, low-wear superlubricity with a shortened running-in period.

At present, research on superlubricity in rolling bearings primarily centered around solid lubricant, including coatings such as diamond-like carbon (DLC), molybdenum disulfide (MoS_2), and graphene-based material [31-34]. These coatings can effectively reduce friction and improve the wear resistance of bearings when operating in a vacuum or nitrogen atmosphere, but they cannot achieve superlubricity in air. In order to verify the superlubricity of diketones in bearing lubrication, we conducted tribological experiments based on angular contact ball bearings. The experimental results showed that the coefficient of friction (COF) and TMR of bearings lubricated with diketone lubricants were significantly reduced by 88.8% and 82.3% respectively compared with commercial lubricants [35]. In addition, the anti-wear performance of the bearing under diketone lubrication was not much different from that of the commercial lubricant, which was much better than that of the bearing under the lubrication of base oils (poly-α-olefins).

According to the previous research results, the superlubricity mechanism of diketone lubricants was primarily attributed to the formation of molecular adsorption films and their synergistic interaction with chelates in the solution [29]. In this work, the critical skidding parameters for the tested angular contact ball bearings were calculated, and both skidding and non-skidding conditions were established to evaluate the tribological behavior using base oil, commercial lubricant, and diketone lubricant. Particular emphasis was placed on the performance of the diketone lubricant under skidding conditions, including verification of adsorption layer formation on the bearing surface. In order to approach the actual application conditions of bearings, start-stop experiments were also conducted under skidding conditions. Finally, the research results showed that compared with base oil and commercial lubricants, diketone lubricants can enable bearings to maintain a lower COF, TMR and wear under skidding conditions, and can enable bearings to maintain an ultra-low COF without running-in when restarted.

2 Materials and methods

2.1 Theoretical analyses

The surface morphology of the bearing is strongly correlated with whether it experiences skidding [41]. In this paper, based on Hertz contact theory, the quasi-static displacement and load distribution of angular contact ball bearings under load were analyzed. Using the Hirano skidding criterion [36, 37], the critical skidding curve was determined, providing a theoretical foundation for selecting experimental parameters in both skidding and non-skidding lubrication tests. It should be noted that although the Hirano criterion was initially derived under dry friction or boundary lubrication conditions, it remains applicable for determining skidding boundaries when lubricants have similar viscosities. In this study, all lubricants had similar kinematic viscosities (approximately 14 mPa·s), thus forming the same elastohydrodynamic lubricating film thickness. Therefore, the differences in skidding behavior primarily stemmed from variations in interfacial shear strength, rather than hydrodynamic effects. Consequently, the Hirano criterion was used as a reliable reference standard for defining skidding and non-skidding test conditions in this study. Based on the outer raceway control theory, the angular contact ball bearing was analyzed under axial and radial loads during high-speed operation. The effects of centrifugal force and gyroscopic torque were also considered. The resulting changes in the relative positions of the bearing components are shown in Fig. 1. The distances from the curvature centers to the final ball center position were represented as $\delta_{ij} = \left(f_i - 0.5\right) \times D + d_{ij}$ and $\delta_{oj} = \left(f_o - 0.5\right) \times D + d_{oj}$. According to Jones ' research, the introduction of Y_{1j} and Y_{2j} variables was conducive to the subsequent solution [38]. According to Fig. 1 and the Pythagorean theorem, the displacement equation can be obtained as: ${Y_{1j}}^2 + {Y_{2j}}^2 - {\delta_{oj}}^2 = 0$ and $\left(B_{1j} - Y_{1j}\right)^2 + \left(B_{2j} - Y_{2j}\right)^2 - {\delta_{ij}}^2 = 0$.

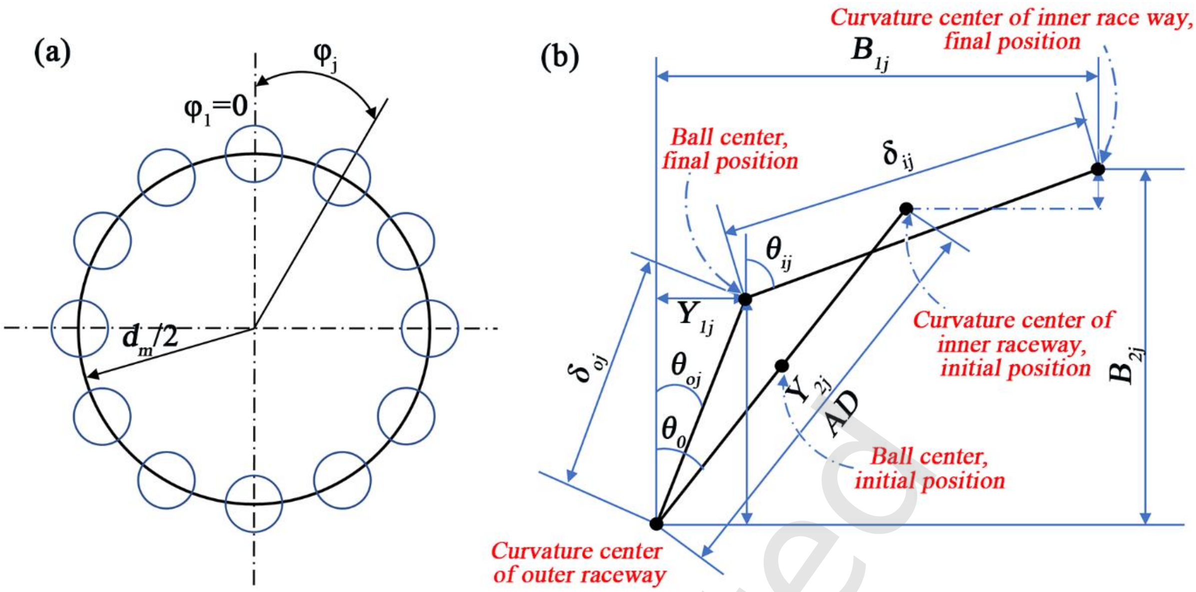

Fig. 1 Geometric configuration of angular contact ball bearings: (a) angular position; (b) schematic illustrating the spatial relationship between the j-th ball and the curvature centers of the raceways.

At high rotational speeds, the double action of centrifugal force and gyroscopic moment, the force acting on the rolling element was shown in Fig. 2, which can be expressed by $\lambda_{ij}=0$, $\lambda_{oj}=2$ [39]. The normal contact force was related to the contact deformation through the relationship $F_{i(o)j}=K_{i(o)j}{d_{i(o)j}}^{1.5}$. Therefore, the force equilibrium equations of the rolling element were:

$$F_{ij}\sin\theta_{ij}-F_{oj}\sin\theta_{oj}+\frac{\lambda_{oj}M_{gj}}{D}\cos\theta_{oj}-\frac{\lambda_{ij}M_{gj}}{D}\cos\theta_{ij}=0 \tag{1}$$

$$F_{ij}\cos\theta_{ij}-F_{oj}\cos\theta_{oj}+\frac{\lambda_{ij}M_{gj}}{D}\sin\theta_{ij}-\frac{\lambda_{oj}M_{gj}}{D}\sin\theta_{oj}+Q_{cj}=0 \tag{2}$$

The rolling element's centrifugal force Q_{cj} and gyroscopic moment M_{gj} were [40]: $Q_{cj}=\frac{1}{2}md_m\omega_m$ and $M_{gj}=J\omega_r\omega_m\sin\beta$.

Where ω_r denoted the rotational angular velocity of the ball, ω_m represented its revolution angular velocity, and β was the attitude angle. ω_r, ω_m and β were given as follows [41]:

$$\omega_r = \frac{\omega \cdot (d_m/D) \cdot (1 - D/d_m \cdot \cos\theta_{ij}) \cdot (1 + D/d_m \cdot \cos\theta_{oj})}{(1 - D/d_m \cdot \cos\theta_{ij}) \cdot \cos(\theta_{oj} - \beta) + (1 + D/d_m \cdot \cos\theta_{oj}) \cdot \cos(\theta_{ij} - \beta)} \tag{3}$$

$$\omega_m = \frac{\omega \cdot \left(1 - D/d_m \cdot \cos\theta_{ij}\right) \cdot \cos(\theta_{oj} - \beta)}{(1 - D/d_m \cdot \cos\theta_{ij}) \cdot \cos(\theta_{oj} - \beta) + (1 + D/d_m \cdot \cos\theta_{oj}) \cdot \cos(\theta_{ij} - \beta)} \tag{4}$$

$$\beta = \arctan(\sin\theta_{oj} / (D/d_m + \cos\theta_{oj})) \tag{5}$$

Rolling bearings were generally composed of multiple balls. After the force state of each ball was obtained, it can be substituted into the equilibrium equation of the bearing's inner ring for further analysis:

$$F_a - \sum_{j=1}^{j=z} \left(F_{ij} \sin\alpha_{ij} - \lambda_{ij} \frac{M_{gj}}{D} \cos\theta_{ij} \right) = 0 \tag{6}$$

With the help of Newton-Raphson method [42], the values of Y_{1j}, Y_{2j}, θ_{ij} and θ_{oj} of each ball were calculated, and then they were brought into the Eq.(6) to obtain the value of d_a. Then the obtained value of d_a was input into Eq.(1) and (2) as the initial value, and Y_{1j}, Y_{2j}, θ_{ij} and θ_{oj} needed to be calculated repeatedly until the compatible value of the primary unknown data d_a was obtained.

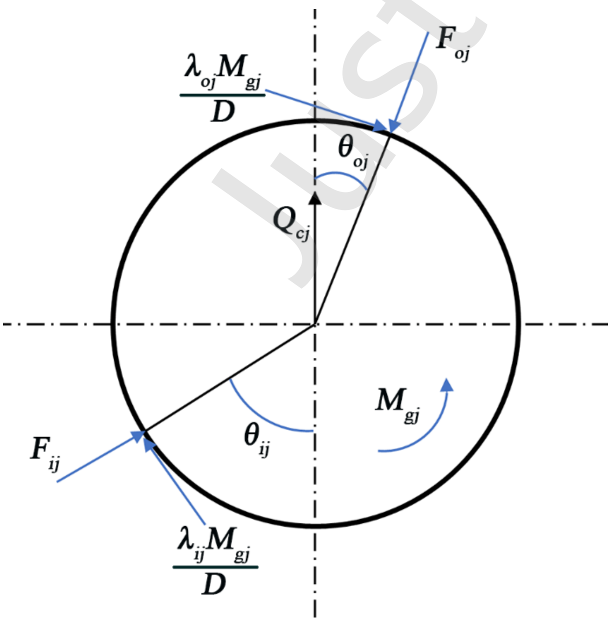

Fig. 2 Force analysis of the ball.

2.2 Materials and lubricants

1-(4-ethylphenyl)-nonane-1,3-dione (0206) was synthesized by Claisen condensation method, and the chelate of diketone and iron (0206-fe) was formed by redox reaction, as shown in Fig. 3. The detailed preparation and purification process can be referred to our previous work [29]. Polyalphaolefin (PAO) was purchased from Tiancheng Meijia Lubricants Beijing Co., Ltd. Previous studies have found that the diketone lubricant PAO=14(20%) obtained by mixing PAO (14 mPa·s) with 0206 and 0206-Fe at mass fractions of 20%, 32% and 48%, respectively, exhibited the best tribological properties [30]. 4112 was commercial bearing lubricants with different viscosities purchased from Sinopec Lubricating Oil Co., Ltd.

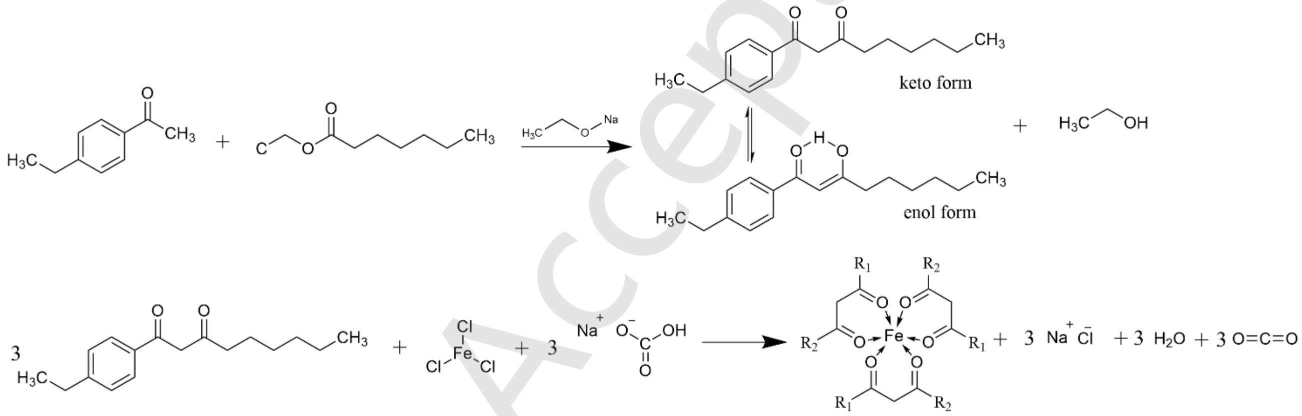

Fig. 3 Preparation principle of diketone and chelate.

2.3 Tribological experiments on bearings

The bearing lubrication test was conducted using a high-speed bearing friction tester (HS-BFT12000) from Lanzhou Huahui Instrument Technology Co., Ltd. Fig. 4 illustrates the core components of the test machine and the bearing assembly process. The bearing outer ring temperature was measured using an OPTRIS Xi 400 infrared thermometer installed on the test machine. Software allowed real-time readings of the bearing outer ring temperature to be synchronized to the high-speed bearing friction test interface and automatically saved after the experiment. During testing, the torque signal from the bearing was captured by a sensor, amplified, and processed via A/D conversion to generate the COF. The torque load sensors have measurement ranges of 0.05~200 mN·m and 0~300 N, respectively, while the machine supports speeds up to 12000 rpm and temperatures up to 150 °C. Prior to testing, both axial load and torque sensors were needed to calibrate using the dedicated tools and standard weights to ensure measurement accuracy.

The bearing used in the tests was a B7004C/P4 model from Luoyang Bearing Research Institute Co., Ltd., with its specifications listed in Table 1. Prior to testing, bearings were ultrasonically cleaned and lubricated with 20 μL of oil applied between the ball and raceways. They were then mounted in a back-to-back configuration. During testing, only axial load was applied. Each sample group underwent a 40-hour test, with lubrication replenished every 10 h following cleaning and disassembly.

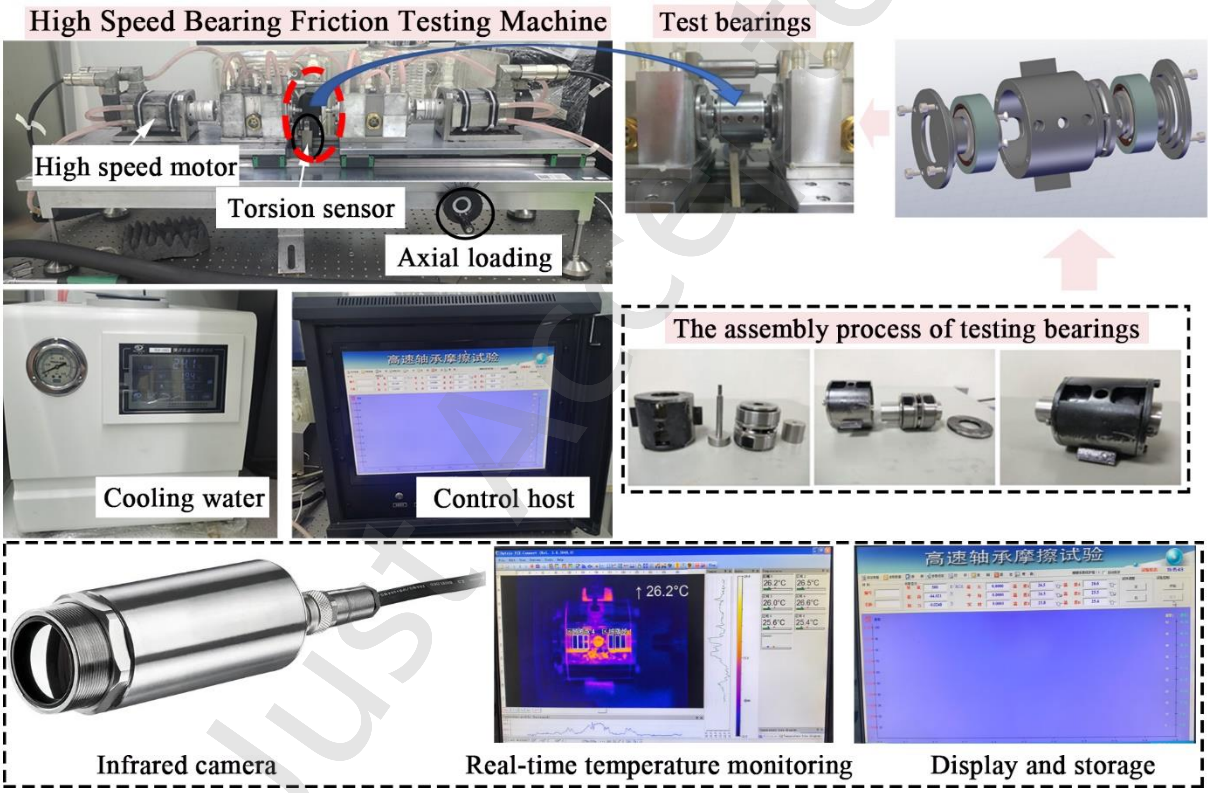

Fig. 4 The physical diagram of high-speed bearing friction testing machine.

Table 1 The parameters of bearing used in tests.

Name	Parameter
Bearing model	B7004C
Accuracy	P4
Material	GCr15
Contact angle	15°

Curvature (f_e, f_i)	f_e=0.54, f_i=0.57
Raceway and ballroughness	0.04 and 0.014 μm
Diameter and number of balls	5 mm and 13

2.4 Surface characterization

Surface analysis was applied to investigate the wear morphology and chemical adsorption characteristics on the ball and raceways, following the bearing lubrication test. The surface topography was observed using scanning electron microscopy (SEM, FEI Quanta 200 FEG) and a 3D white light interferometer (ZYGO NexView). To assess the surface chemical composition and valence states, X-ray photoelectron spectroscopy (XPS, Ulvac-Phi Inc. PHI Quantera II) was employed, utilizing Al Kα radiation at an accelerating voltage of 15 kV and a power of 25 W. The binding energy of C 1s (284.6 eV) served as the reference for energy calibration.

3 Results and discussion

3.1 Bearing skidding prediction

With the increase of bearing speed, skidding occurred when the frictional force at the ball-inner raceway interface was less than the gyroscopic torque. To suppress this phenomenon, increasing the axial load and lowering the rotational speed were effective strategies. Based on experimental studies, Hirano et al. [37] proposed a skidding criterion (Hirano's criterion) for bearings under axial loading. Skidding can be avoided if the following conditions were met:

$$S_f = \frac{F_{ij} \sin\theta_{ij}}{Q_{cj}} > 10 \tag{7}$$

Where, S_f represented the skidding coefficient, and when S_f was greater than 10, it meant that the bearing will not skidding. F_{ij}, θ_{ij} and Q_{cj} in Eq.(7) can be determined by the numerical model. While some more advanced skidding prediction models exist that consider lubrication and COF, these models typically require transient tribological parameters, which are difficult to quantify experimentally in sealed bearing systems. Therefore, the Hirano criterion was adopted here as a simplified yet effective method for identifying skidding. The validity of this assumption was also verified in subsequent bearing surface analysis experiments.

Firstly, the numerical model was verified by comparing with the experimental data of Xu et al [36]. The bearing parameters of B7007C used in the experiment were shown in Table 2. The error between the predicted minimum axial load at 4000-10000 rpm of B7007C to prevent skidding and the experimental data in the reference was within 5.0%, and the data were in good agreement (seen in Fig. 5(a)). Therefore, the above prediction model can be used for the skidding prediction of B7004C/P4 in this study. Here we chose bearing B7004C/P4 as the research object. Based on the established model, the skidding coefficient was evaluated under speeds ranging from 4000 to 10,000 rpm and axial loads between 20 and 100 N. The calculated skidding coefficients were presented in Fig. 5(b). A horizontal line at the threshold value of 10 effectively separated the skidding and non-skidding regions. The results indicated that higher rotational speeds required greater axial loads to suppress skidding. Notably, when the speed exceeded 7000 rpm, skidding occurred across the entire load range. To investigate the lubrication performance under both skidding and non-skidding conditions, experimental parameters were set as follows: 60 N (axial load), rotational speeds 4000 rpm and 8000 rpm. According to Fig. 5(b), the corresponding skidding coefficients are 17.38 and 4.34, respectively, aligning with the intended experimental conditions. In this study, only axial loads were applied to isolate the effects of skidding behavior. Adding additional radial or combined thrust loads would introduce varying contact angles and complex motions, thus obscuring the primary concern regarding lubrication effectiveness; therefore, these conditions will be addressed in future studies.

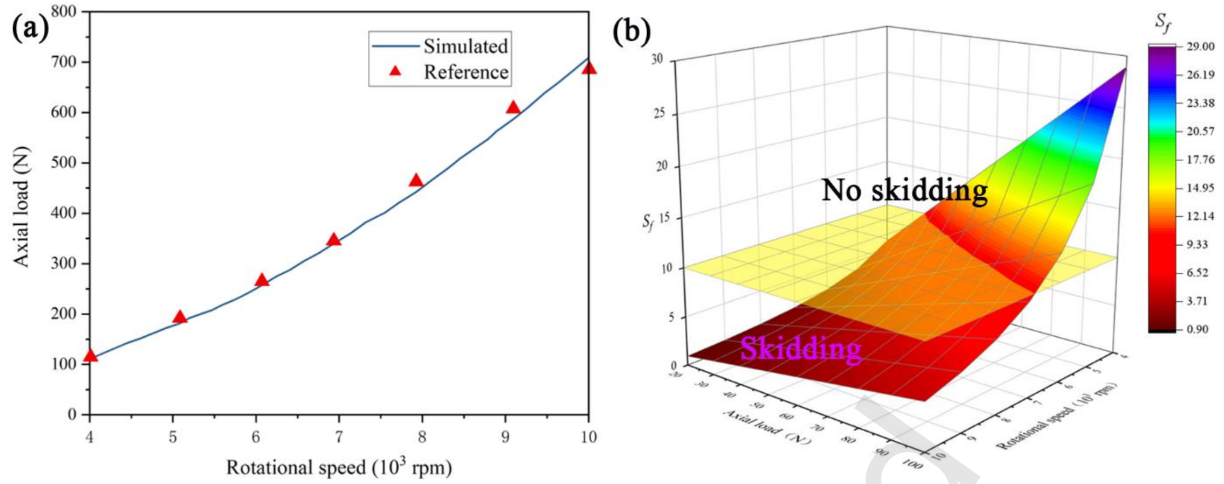

Fig. 5 (a) Minimum axial load to avoid bearing (B7007C) skidding at different speeds obtained through simulation and experiment; (b) the relationship between the skidding coefficient of B7004C and the axial load and rotational speed.

Table 2 The parameters of B7007C for theoretical calculation.

Project	Parameter
Bearing type	B7007C
Inner and outer diameter	35 and 62 mm
Curvature (f_e, f_i)	f_e=0.54, f_i=0.57
Material	GCr15
Contact angle	15°
Pitch diameter d_m	48.5 mm
Contact angle	15°
Diameter and number of balls	6.5 mm and 17

3.2 Friction properies of bearings

Three different types of lubricants with similar viscosities (14 mPa·s), PAO=14, PAO=14(20%) and 4112, were used in the bearing lubrication experimental study. The bearings lubricated by each lubricant were tested under both no-skidding and skidding conditions. The corresponding experimental parameters were 60 N, 4000 rpm and 60 N, 8000 rpm. The effects of different lubricants on the tribological properties and heat generation of bearings under skidding and non-skidding conditions were studied.

Fig. 6 shows the COF and TMR curves of bearings lubricated by base oil, commercial lubricant and diketone lubricant. Each lubricant was tested at 4000 rpm and 8000 rpm, and the experimental results correspond to the first four (black, red, blue and green curves) and last four curves in each figure in Fig. 6. Every sample was tested four times, each test lasting 10 h. After the test, the bearings needed to be ultrasonically cleaned and refilled with 20 μL of lubricant for the next test. Therefore, it can be found that there will be a running-in period in each experiment before the bearing entered a stable lubrication state. Before the start of the experiment, the infrared temperature measuring device measured the temperature of the outer ring to be 26 ℃. The TMR (ΔTemperature) data of the outer ring can be obtained by subtracting the initial 26 ℃ from the outer ring temperature of the actual collected bearing test process, as shown in Fig. 6 (b, d, f).

As shown in Fig. 6(a, c), the COF of PAO=14 and 4112 was higher at 8000 rpm compared to 4000 rpm. A similar trend was observed in the corresponding TMR curves in Fig. 6(b, d). Thie was because the bearing was in a skidding state at 8000 rpm, the sliding friction during the bearing operation accounted for a relatively high proportion, and the bearing had more friction times per unit time at high speed. The COF curves of PAO=14 showed regular sawtooth fluctuations at both speeds, and the values of COF were higher than those of 4112, which indicated that 4112 can improve its anti-friction performance due to the presence of additives. The COF of PAO=14(20%) at 4000 rpm and 8000 rpm were the lowest compared with PAO=14 and 4112, and their average friction coefficients (ACOF) in the stable state were 0.0015 and 0.0008, respectively. It was worth noting that the COF and running-in time of PAO=14(20%) lubricated bearing with skidding behavior was lower than that bearing with non-skidding behavior. This counterintuitive result can be attributed to shear-induced ordering of the diketone molecules: the high shear field during skidding promoted molecular alignment within the confined contact, forming a more uniform and oriented boundary film with reduced shear resistance

[43, 44]. In addition, the maximum TMR of PAO=14(20%) during the running-in period was even higher than that of PAO=14 and 4112 (Fig. 6(f)). After the running-in period, the TMR decreased rapidly, and the average TMR in the stable state was 1.7 ℃ (4000 rpm) and 2.6 ℃ (8000rpm) respectively. The experimental results of PAO=14(20%) can be explained in combination with the diketone superlubricity mechanism proposed in previous studies [30]. Under high speed and high sliding friction conditions, diketone molecules readily reacted with the bearing surface to form an adsorption layer. Meanwhile, chelate molecules in the lubricant helped prevent direct contact between friction pairs and worked synergistically with the adsorption film to achieve rapid friction reduction. Although the COF of the bearing at 8000 rpm under PAO=14(20%) lubrication was lower than that at 4000 rpm, the bearing had more sliding friction times at high speed in the same time, so the heat generated was greater, resulting in a higher TMR of the outer ring of the bearing.

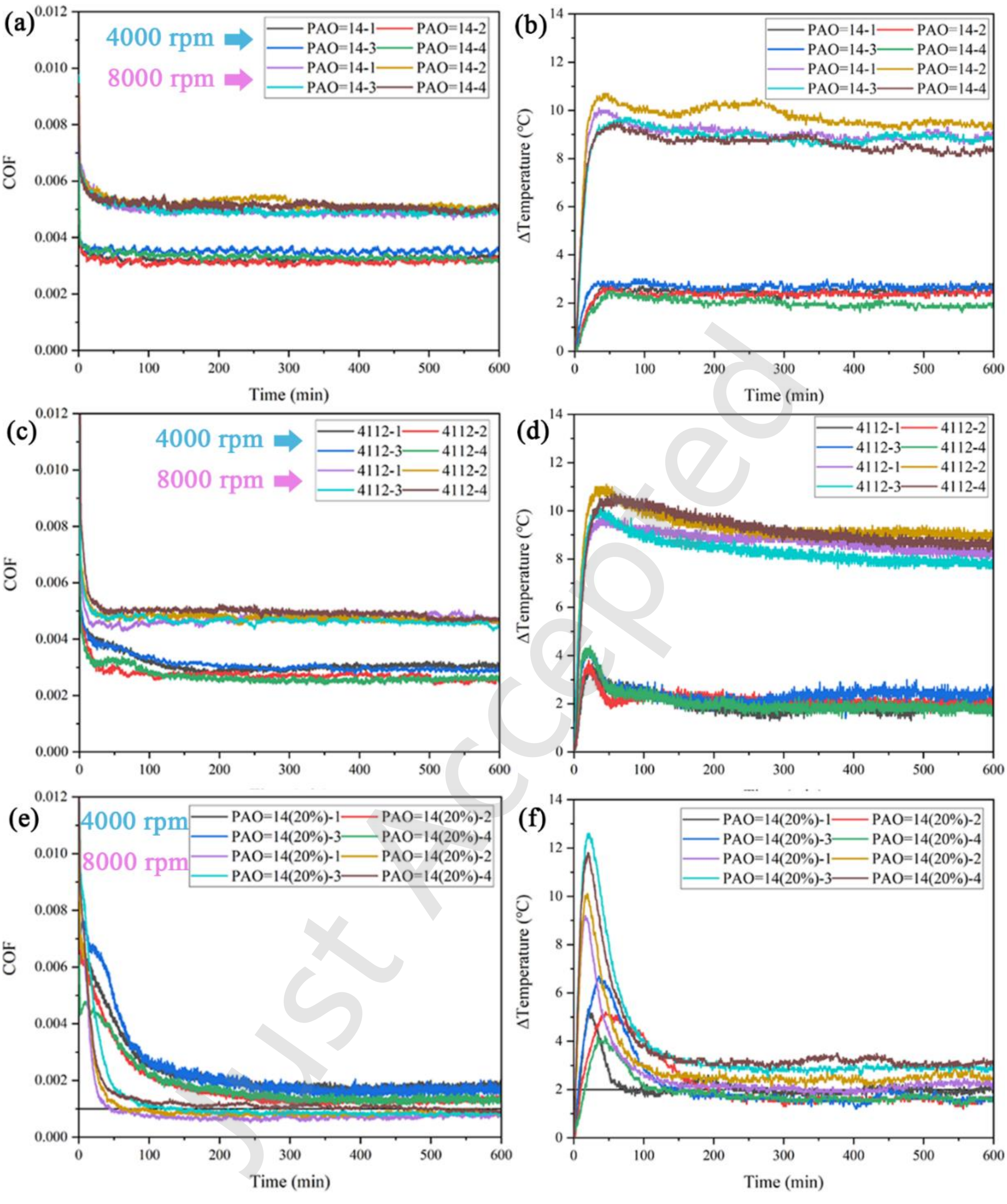

Fig. 6 (a) (c) (e) COF and (b) (d) (f) TMR of bearings lubricated by (a) (b) PAO=14, (c) (d) 4112, and (e) (f) PAO=14(20%) at 60 N, 4000 rpm and 8000 rpm.

3.3 Surface characterization

To assess bearing surface wear under different lubrication conditions, SEM and a 3D white light interferometer were used for surface analysis. SEM was first employed to characterize the micromorphology of the ball, inner raceway, and outer raceway, as shown in Fig. 7. Figure 7 (a1-c1) shows the contrast sample, which has not been tested and can be used as a benchmark for evaluating the severity of bearing wear. Under the condition of 4000 rpm (non-skidding), the bearing lubricated with PAO=14 (Fig. 7 a2-c2) showed moderate abrasive wear, with obvious plowing marks and surface roughening on the ball and raceway, indicating insufficient boundary film formation. In contrast, the commercial lubricant (4112) (Fig. 7 a3-c3) may have formed a tribochemical film due to the presence of additives, which could partially inhibit direct rough contact and improve the surface condition, as further supported by the XPS analysis presented later in this section. However, localized micropitting and abrasive wear indicated that its protective effect was not uniform or completely stable. It was noteworthy that the bearing lubricated with PAO=14(20%) at 4000 rpm (Fig. 7a4-c4) had a smoother surface and minimal surface damage caused by wear. This was due to the strong polarity and surface adsorption ability of the diketone molecules, which helped to form a chemically anchored ordered boundary layer, effectively reducing interfacial shear and preventing metal-to-metal contact. It should be noted that some localized micro-pits observed on the surface of the sphere (Fig. 7(a4)) originated from the early break-in stage and the adsorption film formation process, during which weaker oxidative residues were mechanically removed before a stable adsorption film could form. These shallow pits were not related to fatigue wear, but rather to the adsorption of polar molecules on the surface. At 8000 rpm, significant skidding characteristics were observed: (i) the COF curve increased and fluctuated and the temperature increased was more pronounced compared to 4000 rpm; and (ii) SEM images (PAO=14 and 4112) showed directional micro-scratching and localized shear deformation on the raceway surface, consistent with rolling-slip motion. These results confirm that the bearing was in a skidding state at 8000 rpm. The samples lubricated with PAO=14 showed extensive surface damage, including severe plowing and abrasive wear, which reflected the rupture of the lubricating film and the increase in friction. The performance of 4112 was better than that of PAO, but there were also phenomena such as abrasive wear and adhesive wear, indicating that the lubrication performance was insufficient under high shear. In sharp contrast, PAO=14(20%) can maintain a very smooth surface with negligible wear and can perform well in lubrication even under severe skidding working conditions. This indicated that the tribochemical film formed during its lubrication process can support the load and suppress friction.

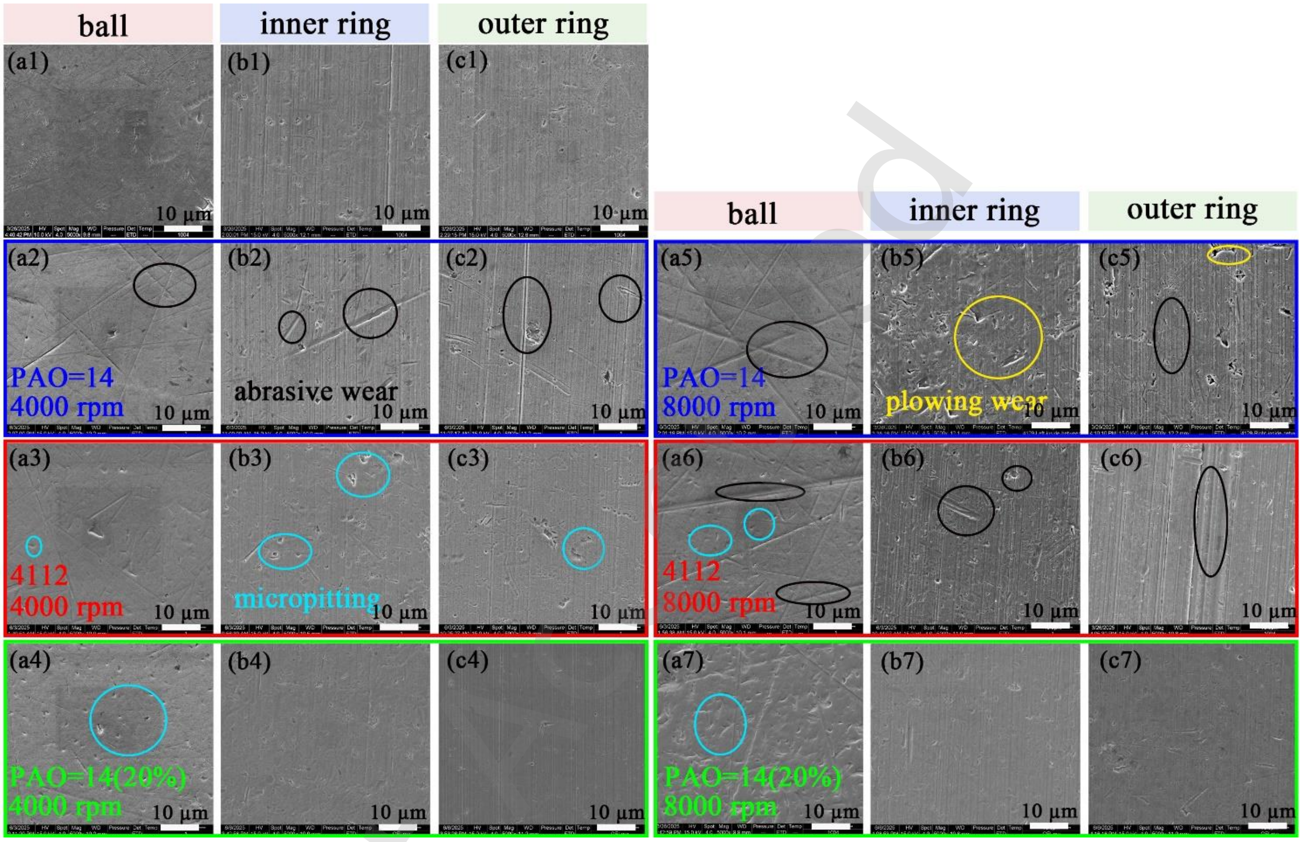

Fig. 7 SEM images of the bearings lubricated with (a2-c2) PAO=14, (a3-c3) 4112, (a4-c4) PAO=14(20%) at 4000 rpm and (a5-c5) PAO=14, (a6-c6) 4112, (a7-c7) PAO=14(20%) at 8000 rpm; (a1-c1) were the contrast sample SEM images.

To further evaluate bearing wear under different lubricants, cross-sections of the raceways were examined using a 3D white light interferometer. As shown in Fig. 8, the surface roughness of raceways lubricated with all three lubricants was higher at 8000 rpm compared to 4000 rpm. This shows that the degree of wear of the bearings running under skidding conditions was more serious than that under no-skidding conditions. Additionally, under identical conditions, the inner ring exhibited greater roughness than the outer ring. This was attributed to the test setup, where the fixed outer ring and rotating inner ring resulted in a higher relative sliding speed-and thus more intense friction-between the ball and the inner ring [45]. This phenomenon will be more obvious at 8000 rpm. Quantitative comparison of the surface line roughness values shows that the roughness of PAO=14(20%) lubricated bearing at 8000 rpm increased by only 22.2% compared with 4000 rpm, while PAO=14 and 4112 increased by 66.7% and 33.3% respectively. This once again proved that diketone lubricants had better anti-wear properties. In addition, it was observed that the cross-sectional profile curves under PAO=14 and 4112 lubrication had a larger fluctuation range, especially at 8000 rpm, where sharp peaks and troughs frequently appeared, which also confirmed the traces of abrasive wear and plowing shown in Fig. 7. The cross-sectional profile of PAO=14(20%) was smoother and showed minimal fluctuations, even lower than the sample's initial surface roughness. This was because the diketone lubricant will grind and polish the surface before achieving superlubricity and form a diketone molecular adsorption film [29], so that the bearing can maintain excellent tribological properties even under skidding conditions.

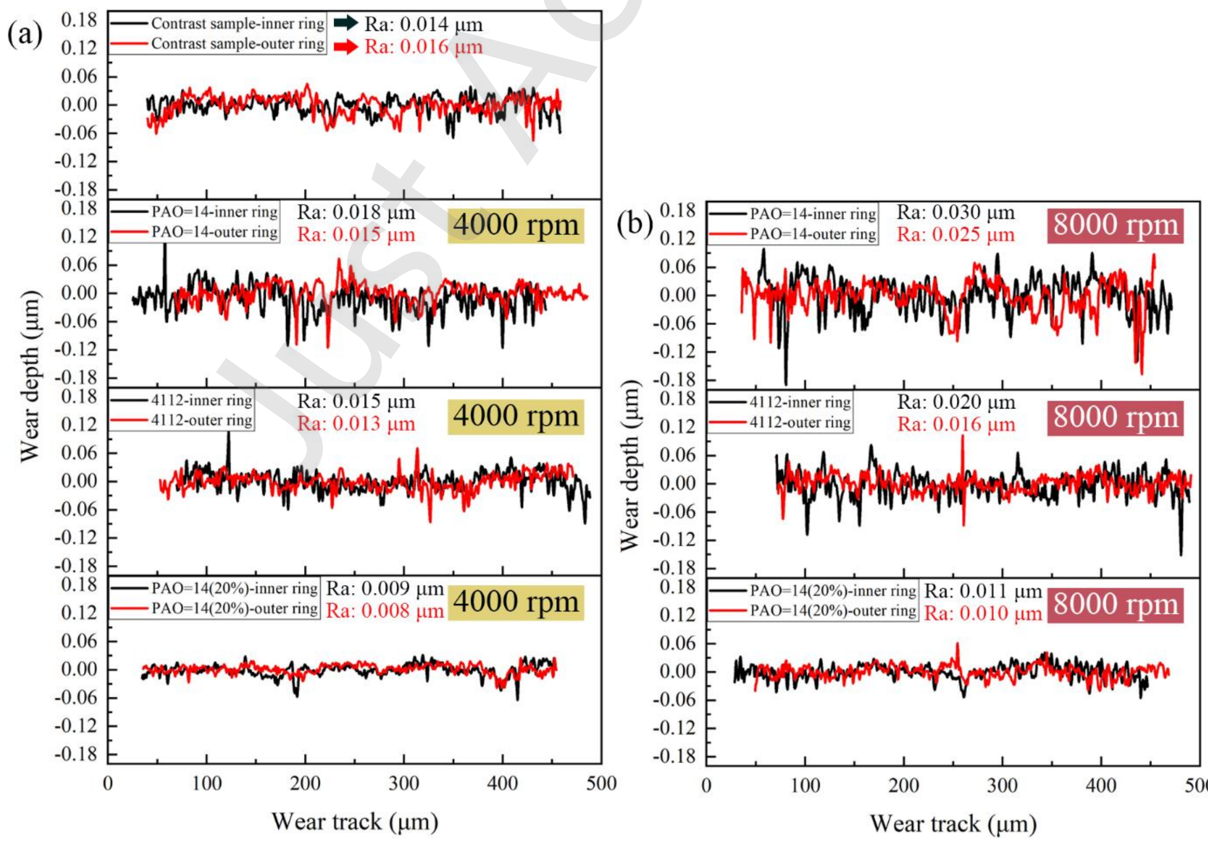

Fig. 8 Cross-sectional profiles of PAO=14, 4112 and PAO=14(20%) lubricated bearings at 4000 rpm and 8000 rpm.

In addition, XPS analysis was used to study the chemical composition and bonding characteristics of the tribofilm formed on the bearing surfaces lubricated with three lubricants: PAO=14, 4112, and PAO=14(20%). As shown in Fig. 9, the C 1s peak of the bearing surface lubricated with PAO=14 mainly corresponded to long-chain aliphatic hydrocarbons (284.8 eV), and the O 1s signal may originated from weak surface oxidation or foreign oxygen-containing species [46, 47]. The appearance of Fe $2p_{3/2}$ and Fe $2p_{1/2}$ with binding energies of 711.0 and 724.6 eV was attributed to the oxidation of surface metals to form Fe_2O_3, among which the peaks with binding energies of 718.8 eV and 729.5 eV were satellite peaks related to Fe $2p_{3/2}$ and Fe $2p_{1/2}$, respectively [48]. The appearance of the iron oxide peak indicateed that the bearing oil film under base oil lubrication was thin and physically adsorbed, with insufficient lubrication and limited surface coverage, thus leading to local rapid oxidation of the bearing surface. In contrast, the 4112 lubricated surface shows additional N 1s and S 2p peaks, indicating the presence of chemically reactive additive residues, likely from nitrogen and sulfur containing antiwear and extreme pressure additives such as ZDDP or thiadiazoles. These additives react tribochemically under load to form protective boundary films composed of metal nitrides (399.2 eV), sulfides (161.7 eV), or oxysulfides (168.0 eV) that helped reduce wear and retard surface fatigue [49, 50]. The presence of such species confirmed that the 4112 additive played an active role in forming interfacial films with tribological benefits. Notably, the PAO=14(20%) sample, although containing only carbon, oxygen, and iron signals, exhibited significantly superior tribological performance in early SEM and cross-section analysis. This was attributed to the formation of a strongly adsorbed chemically bonded film by the diketone additive. The C 1s spectrum may contain a higher proportion of carbonyl-related species (C=O ~288.8 eV), while the O 1s spectrum shows that the C=O bond (530.5 eV) near the benzene ring in the diketone molecule had a lower binding energy than the ordinary C=O bond (532.5 eV) due to the conjugation effect between the benzene and the intramolecular coordination bond [51, 52]. This means that the diketone molecule was chemically adsorbed on the steel surface. The Fe 2p spectrum showed peaks of Fe $2p_{3/2}$ and Fe $2p_{1/2}$ at 710.2 eV and 723.5 eV, and there were no satellite peaks, confirming the formation of Fe_3O_4 on the surface [53]. Despite the lack of traditional heteroatom additives, the diketone lubricant was able to form a uniform, shear-resistant boundary layer that can withstand high-speed and high-load sliding. These results highlight the potential of diketone additives as high-performance, environmentally friendly lubricant components that can replace traditional additives while achieving superior surface protection performance.

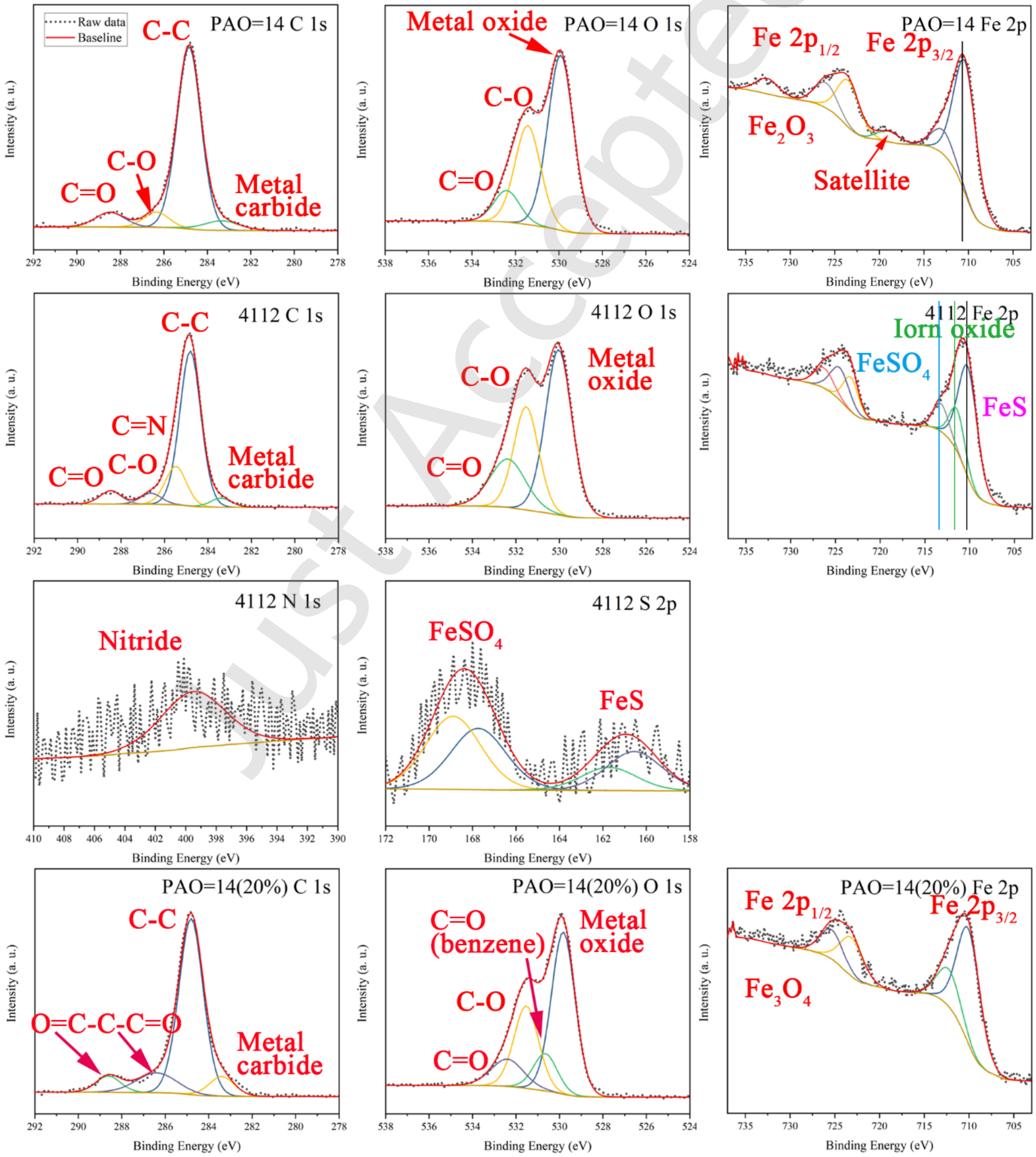

Fig. 9 C 1s, O 1s, and Fe 2p XPS spectra on the surface of the bearing lubricated by PAO=14 and PAO=14(20%); C 1s, O 1s, Fe 2p, N 1s and S 2p XPS spectra on the surface of the bearing lubricated by 4112.

3.4 Lubrication mechanism

To more accurately simulate intermittent bearing operation, start-stop tests were conducted using the above three lubricants. The experimental conditions were 60 N, 8000 rpm, and the duration was 40 h. Each set of experiments had to go through four start-stop states with a time interval of 10 h. As shown in Fig. 10, the ACOF for PAO=14, 4112, and PAO=14(20%) was 0.0052, 0.0044, and 0.0007, respectively. After each restart, PAO=14 and 4112 required a running-in period of approximately 120 min to stabilize the COF, whereas PAO=14(20%) consistently achieved a stable low COF almost immediately, maintaining values below 0.001 over the final 30 h.

Fig. 10(a) further revealed that the instantaneous COF at startup exceeded 0.012 for PAO=14 and 4112 during all four cycles, while PAO=14(20%) exceeded this threshold only on the first cycle, dropping to 0.0025, 0.0019, and 0.0012 in subsequent restarts. The TMR trends of the bearing outer rings mirrored the COF behavior. Bearings lubricated with PAO=14(20%) exhibited the lowest temperature increases, staying below 3 °C even after restart. These results indicated that the diketone adsorption film formed under PAO=14(20%) lubrication remained stable throughout the test. It effectively cooperated with the lubricant to maintain superlubricity and eliminated the need for a running-in period. In contrast, the repeated COF spikes and prolonged stabilization times observed with PAO=14 and 4112 suggested inadequate friction film formation, requiring the surfaces to re-establish contact conditions after each restart. SEM analysis of the bearing surface found that the PAO lubricated surface showed severe abrasive and plowing wear characteristics, while the 4112 lubricant, although it can provide partial protection through the additive-derived friction film, still observed abrasive wear. The bearing surface lubricated by diketone lubricants showed minimal morphological changes and the surface was smooth and continuous. Observation of the cross-sectional profile curves and surface roughness values revealed that the wear tracks on the bearing surfaces lubricated with PAO and 4112 were deeper and more irregular, while the wear tracks on the surface lubricated with diketone lubricant were shallower, more uniform, and had minimal material loss.

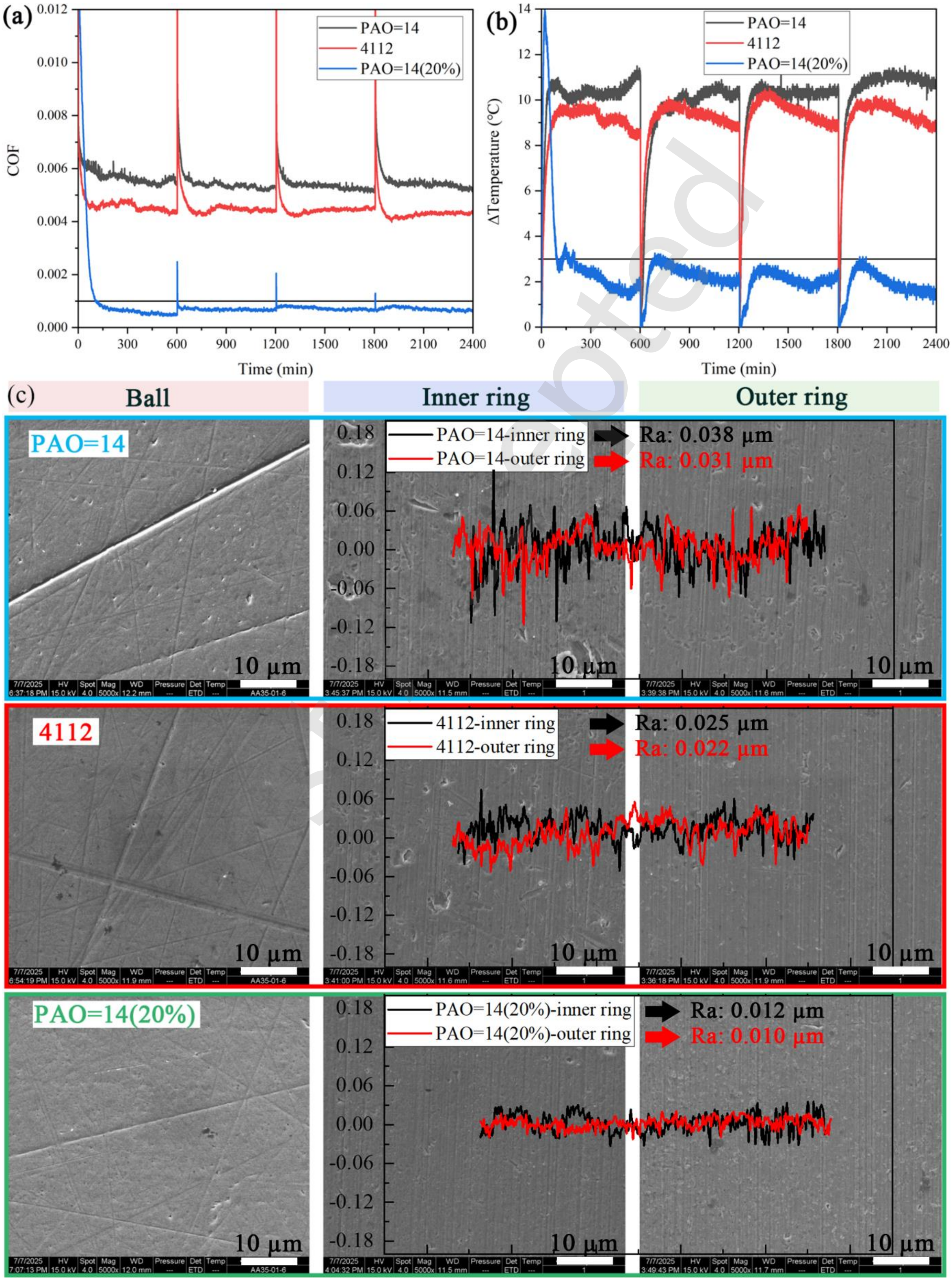

Fig. 10 (a) COF, (b) TMR, and (c) the SEM images and cross-sectional profile of PAO=14, 4112, and PAO=14(20%) lubricated bearing at 60 N, 8000 rpm and four starts and stops.

Based on the experimental results, PAO=14(20%) demonstrated superior tribological performance compared to PAO=14 and 4112 of the same viscosity. Under varying test conditions, the COF and wear of bearings lubricated with PAO=14(20%) remained consistent between skidding and non-skidding states. It is worth noting that achieving ultra-low friction did not necessarily increase the tendency to skidding. The chemically anchored adsorption film and chelate structure in the diketone lubricant enhanced interfacial shear stability and adhesion, thereby maintaining synchronous rolling between the ball and the raceway. Therefore, despite the extremely low COF (< 0.001), the bearing motion remained stable without additional skidding. In contrast, PAO=14 and 4112 showed significantly higher COF and wear under skidding conditions. XPS analysis confirmed the formation of a diketone adsorption film on the bearing surface. Combined with the previously proposed mechanism, this suggested that superlubricity was achieved through the formation of the adsorption film, working synergistically with chelates in the lubricant [30]. This superlubricating state effectively suppressed sliding friction and wear induced by differential motion between the ball and raceway at high speeds. Furthermore, start-stop tests under skidding conditions revealed that bearings lubricated with PAO=14(20%) could re-enter the ultra-low friction state immediately after restart, without requiring a running-in period. This excellent tribological performance was attributed to its ability to form a strong chemically adsorbed tribofilm through polar functional groups, which not only resisted shear-induced degradation but also quickly reformed after relubrication. This durable boundary film contributed to consistent low-friction operation and enhanced cyclic surface protection, indicating that diketone-based lubricants offered a promising alternative for high-reliability bearing applications that required long-term performance stability and resistance to tribo-instabilities during interrupted or cyclic operation.

4 Conclusions

This study first explored the influence of varying loads and speeds on the operating conditions of angular contact ball bearings, with a focus on comparing the tribological performance of base oil, commercial lubricant, and diketone lubricant-all with equal viscosity-under both skidding and non-skidding conditions. Surface characterization and control experiments further confirmed the superior performance of diketone lubricants under skidding. Based on these findings, the following conclusions can be drawn:

(1) Under identical test conditions, PAO=14(20%) lubricated bearing exhibited lower COF and TMR compared to those using base oil or commercial lubricants. Even under skidding, the COF and TMR remained as low as 0.0008 and 2.8 °C, respectively, surpassing the performance of bearings operating non-skidding in terms of both friction and running-in time.

(2) In addition, although the diketone lubricant achieved an ultra-low COF, the formation of a robust chemically adsorbed film effectively stabilized the rolling motion and did not induce additional skidding, ensuring safe and reliable superlubricity operation.

(3) When the bearings lubricated by PAO=14 and 4112 entered the stable operation state under the skidding state, they still needed a running-in period of nearly 120 min after the restart to enter the stable state, while the bearings lubricated with PAO=14 (20%) almost did not need a running-in period to maintain the low COF (0.0007) before the end of the experiment.

(4) The synergistic lubrication mechanism of PAO=14(20%) involved both physical and chemical contributions. The molecules form an oriented adsorption film on the steel surface, while chemical chelation with Fe atoms (0206–Fe) increased its load-bearing capacity, and inhibited direct metal-to-metal contact. The synergistic lubrication mechanism of the diketone adsorption film and the chelate was the main reason for the bearing to maintain an ultra-low COF (0.0008) under the skidding state and achieve superlubricity (0.0007) without running-in after restarting.

Acknowledgements

This work is financially supported by the Fundamental Research Funds for the Central Universities (JB2025019), National Key R&D Program of China (grants no. 2020YFA0711003), the National Natural Science Foundation of China (No. 51925506), and the XPLORER PRIZE.

Declaration of competing interest

The authors have no competing interests to declare that are relevant to the content of this article.

References

(1) Wang, Y.; Wang, W.; Zhang, S.; Zhao, Z. Investigation of skidding in angular contact ball bearings under high speed. Tribol. Int. 2015, 92, 404-417.

(2) Gao, S.; Han, Q.; Pennacchi, P.; Chatterton, S.; Chu, F. Dynamic, thermal, and vibrational analysis of ball bearings with over-skidding behavior. Friction. 2023, 11, 580-601.

(3) Kim, D.; Kin, M.; Ryu, G.; Park, J. On heat, temperature, and cavity oil volume fraction of an under-race lubricated angular contact ball bearing. Tribol. Int. 2023, 187, 108715.

(4) Roy, M. Failure Analysis of Bearings of Aero-Engine. J. Fail. Anal. Prev. 2019, 19, 1615-1629.

(5) Ma, L.; Jiang, B.; Lu, N.; Xiao, L.; Guo, Q. Angular contact ball bearing skidding mechanism analysis and diagnosis considering flexible rotor characteristics. Mech. Syst. Signal. Pr. 2024, 207, 110942.

(6) Dadouche, A.; Kerrouche, R. Bearing skidding detection for high-speed and aero-engine applications. J. Eng. Gas. Turb. Power. 2022, 144(3), 031003.

(7) Han, Q.; Chu, F. Nonlinear dynamic model for skidding behavior of angular contact ball bearings. J. Sound. Vib. 2015, 354, 219-235.

(8) Xie, X.; Xu, J.; Luo J. Analysis of skid damage to cylindrical roller bearing of mainshaft of aeroengine. J. Mech. Sci. Technol. 2020, 34, 3239-3247.

(9) Oktaviana, L.; Tong, V.; Hong, S. Skidding analysis of angular contact ball bearing subjected to radial load and angular misalignment. J. Mech. Sci. Technol. 2019, 33, 837-845.

(10) Zhao, Y.; Ma, Z.; Zi, Y. Skidding and spinning investigation for dry-lubricated angular contact ball bearing under combined loads. Friction. 2023, 11, 1987-2007.

(11) Tu, W.; Shao, Y.; Mechefske, C. An analytical model to investigate skidding in rolling element bearings during acceleration. Biomass Convers. J. Mech. Sci. Technol. 2012, 26, 2451-2458.

(12) Liu, Y.; Wang, W.; Qing, T.; Zhang, Y.; Liang, H.; Zhang, S. The effect of lubricant temperature on dynamic behavior in angular contact ball bearings. Mech. Mach. Theory. 2020, 149, 103832.

(13) Guo, S.; Han, Q.; Zhou, N.; Pennacchi, P.; Chatterton, S.; Qing, T.; Zhang, J.; Chu, F. Experimental and theoretical approaches for determining cage motion dynamic characteristics of angular contact ball bearings considering whirling and overall skidding behaviors. Mech. Syst. Signal. Pr. 2022, 168, 108704.

(14) Yang, F.; Xia, Z.; Ma, X.; Guo, N.; Zhong, Z.; Ye, J. Study on the vibration characteristics of angular contact ball bearing cage under rolling-sliding compound motion. Meas. Sci. Technol. 2024, 35(12), 125125.

(15) Li, J.; Xue, J.; Ma, Z. Study on the thermal distribution characteristics of high-speed and light-load rolling bearing considering skidding. Appl. Sci. 2018, 8(9), 1539.

(16) Fang, B.; Zhang, J.; Wan, S.; Hong, J. Determination of optimum preload considering the skidding and thermal characteristic of high-speed angular contact ball bearing. J. Mech. Des. 2018, 140(5), 053301.

(17) Gao, S.; Han, Q.; Jiang, Z.; Zhang, X.; Pennacchi, P.; Chu, F. Triboelectric based high-precision self-powering cage skidding sensor and application on main bearing of jet engine. Nano Energy. 2022, 99, 107387.

(18) Tang, X.; Li, J. Tribological characteristics of nano-lubricated high-speed rolling bearings considering interaction between nanoparticles and rough surface. Lubricants. 2022, 10(6), 117.

(19) Huang, J.; Tan, J.; Fang, H.; Gong, F.; Wang, J. Tribological and wear performances of graphene-oil nanofluid under industrial high-speed rotation. Tribol. Int. 2019, 135, 112-120.

(20) Hirano, M.; Shinjo, K. Atomistic locking and friction. Phys. Rev. B. 1990, 41(17), 11837-11851.

(21) Hirano, M.; Shinjo, K. Superlubricity and frictional anisotropy. Wear. 1993, 168(1): 121-125.

(22) Hirano, M.; Shinjo, K.; Kaneko, R.; Murata, Y. Anisotropy of frictional forces in muscovite mica. Phys. Rev. Lett. 1991, 67(67), 2642-2645.

(23) Long, Y.; Galipaud, J.; Weihnacht, V.; Makowski, S.; Martin, J. Achieving superlubricity using selected tribo-pairs lubricated by castor oil and unsaturated fatty acids. Tribol. Int. 2022, 169, 107462.

(24) Yuan, Y.; Amann, T.; Xu, Y.; Zhang, Y.; Chen, J.; Yuan, C.; Li, K. Load and velocity boundaries of oil-based superlubricity using 1,3-diketone. Friction. 2023, 11, 704-715.

(25) Basiron, J.; Abdollah, M.; Abdullah, M.; Amiruddin, H. Lubricant mechanisms of eco-friendly lubricant blended with mineral oil for steel-steel contact. Tribol. Int. 2023, 186, 108653.

(26) Wang, Y.; Qiu, Q.; Zhang, P.; Gao, X. Correlation between lubricating oil characteristic parameters and friction characteristics. Coatings. 2023, 13(5), 881.

(27) Amann, T.; Kailer, A. Ultralow friction of mesogenic fluid mixtures in tribological reciprocating systems. Tribol. Lett. 2010, 37, 343-352.

(28) Walter, M.; Amann, T.; Li, K.; Kailer, A.; Ruhe, J.; Moseler, M. 1,3-diketone fluids and their complexes with iron. J. Phys. Chem. A. 2013, 117(16), 3369-3376.

(29) Du, S.; Zhang, C.; Luo, Z. The synergistic effect of diketone and its chelate enables macroscale superlubricity for a steel/steel contact. Tribol. Int. 2022, 173, 107610.

(30) Du, S.; Zhang, C.; Luo, Z. Combination of diketone and PAO to achieve macroscale oil-based superlubricity at relative high contact pressures. Friction. 2024, 12, 869-883.

(31) Vanhulsel, A.; Velasco, F.; Jacobs, R.; Eersels, L.; Havermans, D.; Roberts, E. DLC solid lubricant coatings on ball bearings for space applications. Tribol. Int. 2007, 40(7), 1186-1194.

(32) Cabrera, L.; Gallegos, J.; Lee, S.; Komurlu, M.; Erdemir, A. Tribological behavior of H-DLC and H-free DLC coatings on bearing materials under the influence of DC electric current discharges. Wear. 2023, 522, 204709.

(33) Ge, X.; Chai, Z.; Shi, Q.; Liu, Y.; Wang, W. Graphene superlubricity: A review. Friction. 2023, 11, 1953-1973.

(34) Xiong, L.; Wu, M.; Fan, X.; Zhu, M. Study on the preparation and fretting behavior of bonded oriented MoS2 solid lubricant coating. Friction. 2024, 12, 2505-2518.

(35) Du, S.; Zhang, C.; Luo, Z. Study on the tribological properties of metal rolling bearing under lubrication with diketone lubricants. Sci. China Technol. Sci. 2024, 67, 2003-2017.

(36) Xu, T.; Xu, G.; Zhang, Q.; Hua, C.; Tan, H.; Zhang, S.; Luo, A. A preload analytical method for ball bearings utilising bearing skidding criterion. Tribol. Int. 2013, 67, 44-50.

(37) Hirano, F. Motion of a ball in angular-contact ball bearing. ASLE Transac. 1965, 8(4), 425-434.

(38) Jones, A. A general theory for elastically constrained ball and radial roller bearings under arbitrary load and speed conditions. J. Fluid. Eng-T. ASME. 1960, 82(2), 309-320.

(39) Zhao, Z.; Yin, X.; Wang, W. Effect of the raceway defects on the nonlinear dynamic behavior of rolling bearing. J. Mech. Sci. Technol. 2019, 33, 2511-2525.

(40) Tian, J.; Zhang, C.; Liang, H.; Guo, D. Simulation of the load reduction process of high-speed angular contact ball bearing with coupling model of dynamics and thermos-elastohydrodynamic lubrication. Tribol. Int. 2022, 165, 107292.

(41) Liu, Y.; Chen, Z.; Li, Y.; Zhai, W. Dynamic investigation and alleviative measures for the skidding phenomenon of lubricated rolling bearing under light load. Mech. Syst. Signal Pr. 2023, 184, 109685.

(42) Luo, H.; Li, Y.; Yu, C.; Liu, G.; Mao, X. Numerical and experimental analysis of nonlinear static and dynamic stiffness of angular contact ball bearing. Nonlinear Dynam. 2023, 111, 2281-2309.

(43) Li, K.; Amann, T.; List, M.; Walter, M.; Moseler, M.; Kailer, A.; Ruhe, J. Ultralow friction of steel surfaces using a 1,3-diketone lubricant in the thin film lubrication regime. Langmuir. 2015, 31(40), 11033-11039.

(44) Amann, T.; Kailer, A.; Oberle, N.; Li, K.; Walter, M.; List, M.; Ruhe, J. Macroscopic superlow friction of steel and diamond-like carbon lubricated with a formanisotropic 1,3-diketone. ACS Omega. 2017, 2(11), 8330-8342.

(45) Wang, W., Hu, L., Zhang, S.; Zhao, Z.; Ai, S. Modeling angular contact ball bearing without raceway control hypothesis. Mech. Mech. Theory. 2014, 82, 154-172.

(46) Qiu, J., Wang, Y., Shi, W.; Zhang, C.; Yu, B.; Gao, P.; Bai, Z.; Fan, M. Alkyl germanes: active lubricant additives in PAO-10. Tribol. Int. 2024, 199, 110005.

(47) Zheng, X.; Liu, J.; Du, S.; Zhang, Y. Test and analysis of the tribofilm and surface state during rolling contact under lubrication condition. Tribol. Int. 2023, 187, 108774.

(48) Graata, P.; Somersa, M.; Mittemeijera, E. The initial oxidation of ε-$F_{e2}N_{1}$−x: an XPS investigation. Appl. Surf. Sci. 1998, 136(3), 238-259.

(49) Ma, H.; Li, J.; Chen, H.; Zuo, G.; Yu, Y.; Ren, T. Zhao Y. XPS and XANES characteristics of tribofilms and thermal films generated by two P- and/or S-containing additives in water-based lubricant. Tribol. Int. 2009, 42(6), 940-945.

(50) Nedelcu, I.; Piras, E.; Rossi, A.; Pasaribu, H. XPS analysis on the influence of water on the evolution of zinc dialkyldithiophosphate–derived reaction layer in lubricated rolling contacts. Surf. Inter. Analysis. 2012, 44(8), 1219-1224.

(51) Zhang, S.; Zhang, C.; Chen, X.; Li, K.; Jiang, J.; Yuan, C.; Luo, J. XPS and ToF-SIMS analysis of the tribochemical absorbed films on steel surfaces lubricated with diketone. Tribol. Int. 2019, 130, 184-190.

(52) Zhang, S.; Zhang, C.; Li, K.; Luo, J. Investigation of ultra-low friction on steel surfaces with diketone lubricants. RSC Adv. 2018, 8, 9402-9408.

(53) Jia, J.; Yang, G.; Zhang, C.; Zhang, S.; Zhang, Y.; Zhang P. Effect of magnetic ionic liquid as a lubricant on the friction and wear behavior of a steel-steel sliding contact under elevated temperatures. Friction. 2021, 9(1), 61-74.

Author biography

Shaonan DU. He obtained his Ph.D. degree in mechanical engineering from Tsinghua University, China, in 2024. Now, he is an assistant professor in the School of Energy Power and Mechanical Engineering, North China Electric Power University. His research interests are the oil-based superlubricity and its application.

Chenhui ZHANG. He received his Ph.D. degree in mechanical engineering from Tsinghua University, China, in 2004. Then he has been working at the State Key Laboratory of Tribology at Tsinghua University. From February 2011 to August 2011, he was invited to Luleå University of Technology in Sweden as a visiting scholar. Then he was invited to Weizmann Institute of Science in Israel as a visiting scientist form February 2012 to January 2013. His current position is a professor at Tsinghua University. His research areas cover surface coatings technology and lubrication theory. His current research interest focuses on the superlubricity.

Zhi LUO. He received his Ph.D. degree in organic chemistry from Institute of Chemistry, Chinese Academy of Sciences in 2019. He is currently an assistant professor in CAS Key Laboratory of Engineering Plastics, Institute of Chemistry, Chinese Academy of Sciences. His research interests include the synthesis and application of olefin polymerization catalysts.